6-22-2021

Can improved canopy light transmission ameliorate loss of photosynthetic efficiency in the shade An investigation of natural variation in Sorghum bicolor

Nikhil S. Jaikumar
University of Illinois Urbana-Champaign

Samantha S. Stutz
University of Illinois Urbana-Champaign

Samuel B. Fernandes
University of Illinois Urbana-Champaign

Andrew D.B. Leakey
University of Illinois Urbana-Champaign

Carl J. Bernacchi
USDA ARS

See next page for additional authors

SOCIETY FOR EXPERIMENTAL BIOLOGY

Journal of Experimental Botany, Vol. 72, No. 13 pp. 4965–4980, 2021
doi:10.1093/jxb/erab176 Advance Access Publication 29 April, 2021
This paper is available online free of all access charges (see https://academic.oup.com/jxb/pages/openaccess for further details)

RESEARCH PAPER

Can improved canopy light transmission ameliorate loss of photosynthetic efficiency in the shade? An investigation of natural variation in *Sorghum bicolor*

Nikhil S. Jaikumar[1,†] Samantha S. Stutz[1], Samuel B. Fernandes[1], Andrew D.B. Leakey[1,2,3], Carl J. Bernacchi[1,2,4], Patrick J. Brown[5] and Stephen P. Long[1,2,3,6,*]

[1] Institute for Genomic Biology, University of Illinois at Urbana-Champaign, Urbana, IL 61801, USA
[2] Department of Plant Biology, University of Illinois at Urbana-Champaign, Urbana, IL 61801, USA
[3] Department of Crop Sciences, University of Illinois at Urbana-Champaign, Urbana, IL 61801, USA
[4] USDA ARS Global Change and Photosynthesis Research Unit, Urbana, IL 61801, USA
[5] Department of Plant Sciences, University of California at Davis, Davis, CA 95616, USA
[6] Lancaster Environment Centre, University of Lancaster, Lancaster LA1 4YQ, UK

[†] Current address: Department of Biology, Illinois State University, Normal, IL 61790, USA.
* Correspondence: slong@illinois.edu

Received 15 November 2020; Editorial decision 24 March 2021; Accepted 28 April 2021

Editor: Tracy Lawson, University of Essex, UK

Abstract

Previous studies have found that maximum quantum yield of CO_2 assimilation ($\Phi_{CO2,max,app}$) declines in lower canopies of maize and miscanthus, a maladaptive response to self-shading. These observations were limited to single genotypes, leaving it unclear whether the maladaptive shade response is a general property of this C_4 grass tribe, the Andropogoneae. We explored the generality of this maladaptation by testing the hypothesis that erect leaf forms (erectophiles), which allow more light into the lower canopy, suffer less of a decline in photosynthetic efficiency than drooping leaf (planophile) forms. On average, $\Phi_{CO2,max,app}$ declined 27% in lower canopy leaves across 35 accessions, but the decline was over twice as great in planophiles than in erectophiles. The loss of photosynthetic efficiency involved a decoupling between electron transport and assimilation. This was not associated with increased bundle sheath leakage, based on ^{13}C measurements. In both planophiles and erectophiles, shaded leaves had greater leaf absorptivity and lower activities of key C_4 enzymes than sun leaves. The erectophile form is considered more productive because it allows a more effective distribution of light through the canopy to support photosynthesis. We show that in sorghum, it provides a second benefit, maintenance of higher $\Phi_{CO2,max,app}$ to support efficient use of that light resource.

Keywords: C_4 photosynthesis, crop canopy architecture, food security, leaf form, quantum efficiency, stomata, water use efficiency

Introduction

A major component of crop yield increases over the last century has been increased planting density (Duvick, 2005; Lee and Tolenaar, 2007). The ability to tolerate high planting density depends on a number of morphological traits, including leaf inclination angle (Williams *et al.*, 1968; Tian *et al.*, 2011;). In maize, for example, erectophile plants, with small inclination angles relative to the vertical (i.e. highly erect leaves), are associated with higher grain yield than planophiles (i.e. with drooping leaves and high leaf inclination angles: Pendleton *et al.*, 1968; Lambert and Johnson, 1978; Lee and Tolenaar, 2007; Lauer *et al.*, 2012). Associations between erect leaf angle and higher yield are also found in rice (Sinclair and Sheehy, 1999; Kumagai *et al.*, 2014), wheat (Richards *et al.*, 2019), sugarcane (DaSilva and DeCosta, 2012), and soybean (Jin *et al.*, 2003). In sorghum [*Sorghum bicolor* (L.) Moench], the world's fifth most important cereal crop (Rai *et al.*, 1999), considerable variation exists for leaf inclination angle (Xin *et al.*, 2009) and for further increases in planting density (Xin *et al.*, 2015). A number of genes influencing this trait have been identified (Truong *et al.*, 2015; Xin *et al.*, 2015), and leaf angle is being incorporated as a direct target for improvement through breeding or synthetic biology. However, the causes of the association between erect leaf angle and yield improvement may not yet be fully understood, particularly in canopies of C_4 crops of the Andropogoneae. This tribe includes the highly productive crops: sorghum, sugarcane (*Saccharum officinarum* L.), maize, and the key bioenergy crop giant miscanthus (*Miscanthus*×*giganteus* Greef et Deuter). Therefore there is considerable scope for further work both to improve leaf erectness through selection and to understand better the mechanistic basis for why leaf erectness is linked to improved carbon accumulation by sorghum and related crops.

The most obvious and best studied mechanism by which leaf erectness influences productivity is through directly optimizing light distribution through the canopy (Tian *et al.*, 2011; Gitz *et al.*, 2015). The relationship between light intensity and carbon assimilation is hyperbolic. The uppermost leaves of crop canopies typically experience high light, and gradually approach their asymptotic maximal photosynthetic value (A_{sat}); in contrast, in heavily shaded lower leaves, photosynthesis is light limited and responds linearly to an increase in light. Photosynthetic capacity under strictly light-limited conditions is described by the initial slope of the photosynthetic light–response curve; that is, the maximum quantum yield of carbon assimilation ($\Phi_{CO2,max,abs}$ on an absorbed light basis, $\Phi_{CO2,max,app}$ on an incident light basis). Therefore, increasing light penetration through the canopy is expected to allow more light interception by the lower canopy levels, allowing for a net increase in carbon assimilation at the canopy scale (Srinivasan and Long, 2017). Other mechanisms have also been hypothesized: erect leaves may allow for more efficient shedding of heat (Hunt *et al.*, 2018), while the greater leaf area index (LAI) allowed by erectophile canopies may serve as a nitrogen storage sink (Sinclair and Sheehy, 1999). In addition, the degree to which increased light penetration through erectophile canopies might affect leaf photosynthetic traits, and the extent to which these effects might help explain the observed association between leaf erectness and yield, remains an ongoing topic of research, especially in C_4 species. Previous models of erectophile versus planophile sorghum canopies attributed yield improvements entirely to the direct effects of improved light distribution, and did not take into account potential changes in leaf photosynthetic traits that might accompany changes in canopy architecture (Gitz *et al.*, 2015; Truong *et al.*, 2015). However, the light environment is known to strongly influence the leaf photosynthetic machinery, particularly in the context of self-shading where leaves that develop under high light are gradually subjected to progressively heavier shading as stem and leaf tissue grow above them. Measuring the effects of self-shading on photosynthetic traits might therefore allow for improved predictive power of canopy photosynthesis models, and for a better mechanistic understanding of how increased leaf erectness in sorghum might result in improved productivity.

The extent to which lower canopy leaves may be able to acclimate to progressively heavier shading over their life span constitutes a significant knowledge gap, particularly in the context of the Andropogoneae. In systems such as deciduous forests, lower canopy leaves spend their entire life span in low light, and are known to acclimate to these conditions. Based on ecological theory and experimental evidence (e.g. Syvertsen, 1984), shaded leaves are expected, and found, to invest in thinner leaves, more chlorophyll, a decreased Chl *a*/*b* ratio, and reduced levels of Calvin cycle enzymes. These changes result in lower respiration (R_D), lower light-saturated photosynthetic rate (A_{sat}), unchanged maximal quantum yield of assimilation on an absorbed light basis ($\Phi_{CO2,max,abs}$: Mooney and Gulmon, 1979; Long *et al.*, 1993; Hikosaka and Terashima, 1995), and higher quantum yield on an incident-light basis ($\Phi_{CO2,max,app}$). However, such 'classical' models of shade adaptation are based largely on experiments where leaves experience constant low- or high-light environments. They may not be applicable to situations such as fast-developing crop canopies, in which leaves that begin their lives in high light are subjected to progressively increased self-shading as younger leaves shade older ones, and where shading may affect the microenvironment, in particular light quality such as blue to red ratios. A few studies have found evidence that some C_3 species, under conditions of progressive self-shading, can partially acclimate to shading and potentially maintain high $\Phi_{CO2,max,abs}$. In *Beaucarnia stricta* and *Davallia bullata*, lower canopy leaves exhibit similar $\Phi_{CO2,max,abs}$ to upper canopy leaves (Long *et al.*, 1993). A similar ability to maintain high $\Phi_{CO2,max,abs}$ in the lower canopy is seen in wheat (*Triticum aestivum* L.) crops and wild oat (*Avena fatua* L.; Beyschlag *et al.*, 1990). Upper canopy leaves in *Dryobalanops aromatica* C.F. Gaertn also experience increased self-shading as they age, and

acclimate by trading carbon fixation capacity for increased light-harvesting capacity, while maintaining the same $\Phi_{CO2,max,abs}$ as they age (Ishida *et al.*, 1999). However, evidence from two species of the Andropogoneae indicates that they may not be able to acclimate effectively to self-shading. Lower canopy leaves of maize and giant *Miscanthus* were found to have 14–15% and 27–29% lower $\Phi_{CO2,max,abs}$, respectively, compared with upper canopy leaves (Pignon *et al.*, 2017). These results were shown to be effects of shade rather than leaf age, based on comparisons between exposed leaves at the southern edge of stands, with similarly aged shaded leaves within the interior of the stands (Collison *et al.*, 2020). Quantum yield decline in the lower canopy, in maize and miscanthus, might be linked to the difficulties of coordinating CO_2 uptake by phosphoenolpyruvate carboxylase (PEPC) in the mesophyll and by Rubisco in the bundle sheath. Bundle sheath leakiness (ϕ) is known to increase with declining light (Kromdijk *et al.*, 2008; Tazoe *et al.*, 2008), which could lead to decreases in the productivity and efficiency of photosynthesis in the lower canopy. However, previous studies on the photosynthetic effects of self-shading in the Andropogoneae have considered only one or two genotypes of the species examined, and studies in sugarcane have found a similar effect in one genotype, but no effect on quantum yield in another (Marchiori *et al.*, 2014). Therefore, it remains a topic for further inquiry, whether quantum yield decline under self-shading is broadly present within the germplasm of a species and across the Andropogoneae.

In a set of field studies across 4 years, the effect of self-shading on photosynthetic performance in lower canopy sorghum leaves was studied. Carbon assimilation, electron transport, stomatal conductance, and activity of three key C_4-specific photosynthetic enzymes were compared between upper and lower canopy leaves, within a genetically diverse range of accessions varying widely in canopy architecture and thereby in the degree of self-shading. Accessions with erect leaves and high light transmission through the canopy are henceforth referred to as 'erectophile' and those with low leaf erectness as 'planophile'. In the final year of the study, bundle sheath leakiness in erectophile and planophile accessions was also compared. The objectives of this study were 3-fold: (i) to test the hypothesis that quantum yields would decrease in the lower canopy of a wide range of sorghum genotypes; (ii) to test the hypothesis that erectophile genotypes, that allow improved light penetration through the canopy, would show a smaller loss of photosynthetic efficiency in the lower canopy leaves; and (iii) to test whether bundle sheath leakiness would increase and concentrations of C_4 enzymes needed to support the light-saturated rate of photosynthesis would decline in the lower canopy leaves. All three hypotheses were supported. The erectophile form is known to allow a more effective distribution of light, thereby supporting higher canopy-level photosynthesis. Here we show that a secondary benefit is that it allows the lower leaves to maintain higher quantum yields, so further boosting canopy carbon gain and productivity.

Materials and methods

Planting conditions

A biomass sorghum diversity panel previously reported in genetic studies by Valluru *et al.* (2019) and dos Santos *et al.* (2020) was used for this study. In summary, the panel was composed of 869 photoperiod-sensitive sorghum accessions that do not flower at our study location and are referred to as biomass or fiber accessions. The panel consisted of 3% bicolor, 18% caudatum, 22% durra, 21% guinea, 1% kafir, and 35% mixed-ancestry accessions. Geographic collection sites ranged worldwide, although the most common sources were Mali and Ethiopia. The diversity panel was planted in 2016 and 2017 at two sites: Savoy, IL (Fisher Farm in 2016: 40.02°N, 88.24°W and Maxwell Farm in 2017: 40.04°N, 88.24°W) and Urbana, IL (Energy Farm in all years: 40.06°N, 88.19°W). Soils at the Savoy sites are fine-silty mixed mesic Typic Endoaquolls and at the Urbana site fine montmorillonitic, mesic Aquic Argiudolls. Each accession was planted in a four-row plot (one plot per site) randomized in an augmented block design, as described in dos Santos *et al.* (2020). Plots consisted of a row length of 3.0 m, with 1.5 m alleys and 0.76 m between rows within a plot. Target density was ~270 368 plants ha^{-1}. Seeds were treated with fluxofenim safener and mefenoxam fungicide before planting. Plots were planted in late May using a four-row planter attached to a tractor. (*S*) metolachlor herbicide was applied during the growing season. Plants were harvested in early October using a four-row small plot harvester (Kemper Head 5830: John Deere, Moline, IL, USA). Over the period 15 May–30 September, total precipitation was 569 mm in 2016, 309 mm in 2017, 572 mm in 2018, and 436 mm in 2020: mean temperature was 23.2 °C in 2016, 22.2 °C in 2017, 23.1 °C in 2018, and 21.9 °C in 2020; and daytime highs exceeded 32 °C on 25 d in 2016, 26 d in 2017, 32 d in 2018, and 24 d in 2020. The core photosynthetic traits were measured at both sites in 2016 and 2017. Canopy extinction coefficients were measured in 2018 and 2020, leaf absorptance in 2018, and bundle sheath leakiness in 2020. Levels of C_4 mesophyll cycle enzymes were measured in 2017 and Rubisco content was measured in 2020.

Screening for leaf inclination angle

All accessions were screened for leaf inclination angle, manually with protractors, between 5 and 22 July 2016 and between 26 June and 14 July 2017. Leaf inclination angle is defined here as the angle of the leaf at the point of insertion relative to the vertical. The assumption, subsequently tested, was that leaf inclination angle would be a proxy for canopy light transmission. Leaf inclination angle was assessed at the base of the lamina, from the ligule and point of attachment to the sheath. Both the youngest fully expanded leaf (i.e. the youngest showing ligule emergence) and the oldest fully green leaf were measured for three plants of each of the 869 accessions at each site. Accessions with extreme phenotypes—the 40 with the lowest and 40 with the highest leaf inclination angles relative to the vertical—were identified. Because inclination angles of the youngest fully expanded leaf and oldest fully green leaf were moderately correlated in 2016 (r^2=0.32, P<0.0001) and in 2017 (r^2=0.60, P<0.0001), only the youngest fully expanded leaf was used to identify accessions of interest. Erectophile accessions are defined as having leaf inclinations relatively close to the vertical (low inclination angle at the youngest fully expanded leaf) and planophile accessions as having relative inclinations close to the horizontal (high inclination angle). From this subset of 80 extreme phenotypes, 10 erectophiles and eight planophiles were selected at random for photosynthetic trait analysis in 2016, after removing those with high coefficients of variation (>0.33), and 12 erectophiles and nine planophiles were selected following the same procedure in 2017. Across the two years, 18 erectophile and 17 planophiles were represented, since four erectophile accessions overlapped between the two years. The accessions in 2018 were taken from the erectophile and planophile ends of the 2017 screening, and mostly overlapped with the accessions that had

been chosen for photosynthesis in 2017; as three lines were missing due to inadequate seed quantity (two planophile and one erectophile), three alternative lines were substituted, comprising 18 erectophiles and 17 planophiles. In 2020, the measurement of canopy light profiles involved 24 accessions (12 erectophile and 12 planophile) comprising most of the 2016 and 2017 accessions. Since not all of the previous years' lines were available due to inadequate seed quantity, five others (all erectophiles) were chosen randomly from the 2017 angle screening and added to the study to compensate for missing accessions

Light environment

To verify that leaf erectness influenced light distribution through the canopy, photosynthetic photon flux density (PPFD, herein referred to as '*Q*') in the canopy was measured with a 1 m line quantum sensor (Decagon Devices: Pullman, WA, USA) to provide a spatially averaged photon flux at two heights within the canopy: at the youngest fully expanded leaf near the top of the canopy and at the lowest fully green leaf. Measurements of *Q* were made on 7 August 2016 and 12 August 2017. In addition, full canopy light profiles were measured on 15 July and 12 August 2018, on the same set of accessions that had been chosen for photosynthetic sampling in 2017. Here, light was measured at the top of the canopy, defined as height=1, and then at heights of 0.75, 0.5, 0.25, and 0.1 of the distance from the ground (0) to the top of the canopy. Extinction coefficients (*k*) were determined as follows:

$$Q_Z = Q_0 e^{-kZ}$$

where Q_0 = incident light above the canopy and Z = depth into the canopy.

On 14 July 2020, extinction coefficients were measured again, this time based on six data points, at the canopy surface and then at relative distances of 0.8, 0.6, 0.4, 0.2, and 0.1 from the ground (0) to the top of the canopy (1).

Photosynthetic light–response curves for accessions from the diversity panel

Leaf photosynthetic traits were measured with portable infrared CO_2/water vapor gas exchange systems each with a modulated chlorophyll fluorometer integrated into its leaf cuvette (LI-6400 XT, LI-COR, Lincoln, NE, USA). The Savoy site was sampled from 4 to 10 August 2016 and from 21 to 25 August 2017: the Urbana site was sampled from 12 to 18 August 2016 and from 10 to 18 August 2017. For each accession, sun leaves and shade leaves were collected at dawn. The cut ends were placed in water and immediately re-cut under water to allow the water column to re-fill, following Pignon *et al.* (2017). This procedure avoided confounding photosynthetic capacity with diurnal changes in leaf water potential and temperature, as well as any transient photoinhibition or feedback inhibition from accumulation of non-structural carbohydrates over the course of the day. The youngest fully expanded leaf was used to typify 'sun' leaves and the oldest fully green leaf (i.e. with no sign of senescence or significant damage) to typify 'shade' leaves.

Cut leaves were transported to the laboratory where leaves were clamped into the cuvette of the gas exchange system. Cuvette conditions were 30 °C block temperature, Q=2000 μmol m^{-2} s^{-1}, and $[CO_2]$=400 μmol mol^{-1}, with a water vapor pressure deficit of 1.27–1.91 kPa. Once steady state (variation of <3% over 1 min) was achieved, the response of photosynthesis to light was determined. Gas exchange and fluorescence parameters were measured at Q=2400, 2000, 1600, 1200, 800, 600, 400, 300, 250, 200, 150, 100, 80, 60, 40, and 20 μmol m^{-2} s^{-1}. The multiphase flash fluorescence (MPF) protocol (Loriaux *et al.*, 2013) was used to estimate maximum chlorophyll fluorescence in the light (F_m') from which PSII efficiency (Φ_{PSII}) and the ratio of variable to maximal fluorescence in the light (F_v'/F_m') was calculated. The 900 ms long MPF intensity was 8000 μmol m^{-2} s^{-1} with a 20% phase 2 ramp. To calculate photosynthetic traits on an absorbed light basis, leaf absorptance (α) was determined using an integrating sphere and scanning spectrometer (JAZ, Ocean Optics: Largo, FL, USA) coupled with the SpectraSuite software, on parallel leaf samples collected from the same accessions in 2018. This allowed the conversion of measured incident light (*Q*) to light absorbed by the leaf (Q_{abs}).

Light–response curves were fit by non-linear regression (NL procedure in STATA 15.1: StataCorp, College Station, TX. USA). Light–response curves were modeled as a non-rectangular hyperbola, with Equations 2, 3, and 4 describing assimilation, electron transport, and stomatal conductance, respectively.

$$A = \{A_{sat} + \Phi_{CO2,max,app}\, Q - [(A_{sat} + \Phi_{CO2,max,app})^2 - 4A_{sat}\, \Phi_{CO2,max,app}\, \theta Q]\}^{0.5}/[2\theta_A] - R_D$$

$$J = \{J_{max} + \Phi_J\, Q - [(J_{max} + \Phi_J)^2 - 4J_{max}\, \Phi_J\, \theta Q]\}^{0.5}/[2\theta_J]$$

$$G_S = \{G_{S,max} + \Phi_G\, Q[(G_{S,max} + \Phi_G)^2 - 4G_{S,max}\, \Phi_G\, \theta G]\}^{0.5}/[2\theta_G]$$

Here A_{sat}, J_{sat}, and $G_{S,sat}$ represent light-saturated values, and $\Phi_{CO2,max,abs}$, Φ_J, and Φ_G represent light-limited quantum yields, namely initial slopes of assimilation, electron transport, and stomatal conductance against light, respectively. The parameter R_D represents light-adapted respiration, G_0 represents stomatal conductance at zero light, and θ is a convexity parameter. To gain better precision for our estimates of quantum yield of gas exchange ($\Phi_{CO2,max,abs}$) and quantum yield of electron transport (Φ_J), linear regressions were separately conducted on the initial portion of the curve; that is, Q<100–150 μmol m^{-2} s^{-1}. The exact range, for each plant, was chosen to optimize r^2 for this initial linear portion (Long *et al.*, 1993). Initial slopes for the *A* versus *Q* response were calculated on an incident light basis (apparent quantum yield, $\Phi_{CO2,max,app}$). Dividing this value by leaf absorptance (α) gave quantum yield on an absorbed light basis ($\Phi_{CO2,max,abs}$). Quantum yield of electron transport (Φ_J) was estimated from ΦPSII measurements, using Equation 5 and assuming a partition of 0.4 between PSII and PSI (Edwards and Baker, 1993),

$$J = 0.4\ \alpha Q\,(\Phi PSII)$$

Constraints for the model were R_D >0.3, G_0 >0.01, and 1>θ>0.01.

Q values from field measurements described above were combined with parameters extracted from light–response curves, to estimate leaf-level carbon assimilation under ambient light conditions ($A_{ambient}$) as well as analogous estimates for electron transport ($J_{ambient}$) and intrinsic water use efficiency ($IWUE_{ambient}$). Here, 'ambient' refers to the light environment that sun and shade leaves were actually experiencing in the field at midday, on sunny days in late summer after full canopy closure. The import of these estimates is to simulate carbon assimilation, electron transport, and water use efficiency under field conditions, and to gain information about how the effects of changes in leaf-level photosynthetic traits and canopy light environments might compound one another. To calculate, $A_{ambient}$, $J_{ambient}$, and $IWUE_{ambient}$ for shade leaves of a particular accession (e.g. 'Doronko'), the light intensity values measured in the field for upper and lower canopy *Q* were substituted in Equations 2, 3, and 4, respectively, using the parameters estimated from light–response curves (Φ_{CO2}, A_{sat}, etc.) for 'Doronko' shade leaves, as well as measured values of absorptance (α).

Leakiness (ϕ) in upper and lower canopy leaves

Upper and lower leaves (youngest fully expanded leaf and oldest fully green leaf) from erectophile and planophile accessions were excised from the plants in the field at dawn: the cut ends were immediately placed in water and cut again under water to allow the water column

to re-fill. Leaves were cut between 05.30 h and 06.30 h from 18 to 26 August 2020. Cut leaves were taken to the lab and remained with cut ends continuously under water, in the dark, until photosynthesis was measured.

Leaves were placed in a controlled-environment plant growth cabinet (Gen 1000, Conviron Controlled Environments, Winnipeg, Canada) with a Q of ~700 μmol m^{-2} s^{-1} and 35 °C for ~5 min before being placed in the large flat leaf chamber of a LI-6800 (LICOR Biosciences) located in the growth cabinet. Leaf temperature was set to 35 °C, Q to 2200 μmol m^{-2} s^{-1}, [CO_2] to 400 μmol mol^{-1}, and chamber relative humidity to 50% with 21% [O_2]. Leaves were allowed to acclimate while the rate of photosynthesis and stomatal conductance increased to a steady state, requiring 20–35 min. After ~30 min, irradiance was decreased to 80 μmol quanta m^{-2} s^{-1}. Once photosynthesis stabilized under 80 μmol quanta m^{-2} s^{-1}, the LI-6800 was matched and the plant was allowed to photosynthesize for another 30 min. The LI-6800 was coupled to a tunable diode laser absorption spectroscope (TDL; model TGA 200A, Campbell Scientific, Inc., Logan, UT, USA) measuring $^{12}CO_2$, $^{13}CO_2$, and $\delta^{13}C$ (Bowling *et al.*, 2003; Pengelly *et al.*, 2010; Ubierna *et al.*, 2013, 2017). Input gases (N_2 and O_2) were mixed using mass flow controllers (Omega Engineering Inc., Norwalk, CT, USA) linked to a datalogger and a voltage output module (CR1000 and SDM-CV04, Campbell Scientific, Inc.). A portion of the N_2/O_2 stream was passed to the LI-6800 while the remainder was used to correct for drift in the TDL over the course of the measurements. The TDL was calibrated by diluting a 10% CO_2 tank in the N_2/O_2 stream to produce four different [CO_2] of the same isotopic composition (Tazoe *et al.*, 2009; Pengelly *et al.*, 2010; Ubierna *et al.*, 2013). The measurement sequence consisted of a zero [CO_2] and three [CO_2], a calibration tank with a known [$^{12}CO_2$], [$^{13}CO_2$], and $\delta^{13}C$ composition, followed by the LI-6800 reference, and a sample leaf chamber. The TDL measured each of the six gas streams for 20 s. The LI-6800 was set to autolog every 140 s, once per TDL measurement cycle. The TDL was connected to the LI-6800 reference using the reference port on the back of the LI-6800 head. The port on the front of the LI-6800 was used for measuring the [$^{12}CO_2$], [$^{13}CO_2$], and $\delta^{13}C$ composition of the leaf chamber air.

Calculations of photosynthetic discrimination ($\Delta^{13}C$) and estimation of bundle sheathleakiness (ϕ) under high light

Online photosynthetic discrimination ($\Delta^{13}C_{obs}$) was calculated according to Evans *et al.* (1986):

$$\Delta\ ^{13}C_{obs} = \frac{1000\xi(\delta^{13}C_{samp} - \delta^{13}C_{ref})}{1000 + \delta^{13}C_{samp} - \xi(\delta^{13}C_{samp} - \delta^{13}C_{ref})}$$

where $\delta^{13}C_{samp}$ and $\delta^{13}C_{ref}$ are the carbon isotope compositions of the leaf chamber and reference air in the LICOR and where ζ is:

$$\xi = \frac{C_{ref}}{(C_{ref} - C_{samp})}$$

where C_{ref} and C_{samp} are the CO_2 concentrations of dry air entering and exiting the leaf chamber, respectively, measured by the TDL.

The enzyme-limited estimate of leakiness, including the ternary effect (t) (Farquhar and Cernusak, 2012), under high irradiance was estimated using the model proposed by Ubierna *et al.* (2013):

$$\phi_{HL} = \frac{\frac{(1-t)\ \Delta\ ^{13}C_{obs}C_a - a'\ (C_a - C_i)}{(1+t)C_i} - b_4'\ + \frac{e'R_m}{A+0.5R_D}}{b_3' - s + e'\ \left(\frac{R_m}{A+0.5R_D} - \frac{R_D}{A+R_D}\right)}$$

where, C_a and C_i are the ambient and intercellular CO_2 partial pressure, respectively. The fractionation during leakage from the bundle sheath cells (s) is 1.8‰, b'_3 (29‰) is the Rubisco fraction, and b'_4 (–4.7‰) is the net fractionation by CO_2 dissolution, hydration, and PEPC activity at 35 °C (Farquhar, 1983; Henderson *et al.*, 1992; von Caemmerer *et al.*, 2014). R_D is leaf mitochondrial respiration in the light, R_m (R_m=0.5R_D) is the rate of mesophyll cell respiration in the light, and A is the rate of photosynthesis. The fractionation during decarboxylation including measurement artifacts (e') is estimated according to Wingate *et al.* (2007):

$$e'\ = e + \ \delta^{13}C_{ref} - \delta^{13}C_{gatm}$$

where e is the respiratory fractionation during decarboxylation, $\delta^{13}C_{ref}$ is the isotopic signature of the CO_2 entering the LICOR reference, and $\delta^{13}C_{gatm}$ is the isotopic signature of the CO_2 where the plants are grown, –8‰ in our study.

The ternary effect (t) (Farquhar and Cernusak, 2012) takes into account the carbon isotope discrimination on the rate of CO_2 assimilation and is calculated as:

$$t = \frac{(1 + a')\,E}{2g^t_{ac}}$$

where, E is the rate of transpiration and g^t_{ac} is the total conductance to CO_2 diffusion including boundary layer and stomatal conductance (von Caemmerer and Farquhar, 1981) and a' denotes the combined fractionation factor through the leaf boundary layer and stomata:

$$a' = \frac{a_b\,(C_a - C_L) + a_s(C_L - C_i)}{(C_a - C_i)}$$

where C_L is the leaf surface CO_2 partial pressure, a_b (2.9‰) is the fractionation occurring through diffusion in the boundary layer, and a_s (4.4‰) is the fractionation due to diffusion in air (Evans *et al.*, 1986).

Estimation of bundle sheath leakiness (ϕ) in low light.

For our estimates of ϕ under low light, we assumed that mesophyll conductance was infinite (C_i=C_m), based on the modeling of Ubierna *et al.* (2011) which demonstrated that the effects of g_m on C_4 photosynthetic discrimination calculations under low light were small. We also assumed a constant bundle sheath conductance (g_{bs}) following Brown and Byrd (1993). Leakiness under light-limited conditions was then calculated according to Ubierna *et al.* (2013):

$$\phi_{LL} = \frac{1}{C_i}\frac{\Delta\ ^{13}C_{obs}\,(1-t)\,C_a - a'\,(C_a - C_i) - (1-t)C_i b_4}{(1+t)(b_3 - s)}$$

where, b_3 is the ^{13}C fractionation during carboxylation by Rubisco including respiration and photorespiration, and b_4 is the net fractionation by CO_2 dissolution, hydration, and PEPC including respiratory fractionation:

$$b_3 = b_3'\ - \frac{e'R_D}{V_c} - \frac{fV_o}{V_c}$$

and

$$b_4 = b_4'\ - \frac{e'\ R_m}{V_p}$$

where, b'_3 (30‰) and f (11.6‰) are the ^{13}C fractionation during carboxylation by Rubisco (Roeske and O'Leary, 1984) and ^{13}C fractionation during photorespiration (Lanigan *et al.*, 2008), respectively. The changes in net fractionation by CO_2 dissolution, hydration, and PEP carboxylation including respiratory fraction (Farquhar, 1983; Henderson *et al.*,

1992), b'_4, with temperature were calculated at 35 °C according to von Caemmerer *et al.* (2014):

$$b'_4 = \frac{-9.483 \times 1000}{273 + (T°C)} + 23.89 + 2.2$$

V_c, V_o, and V_p are the rate of Rubisco carboxylation, Rubisco oxygenation, and PEP carboxylation, respectively (von Caemmerer, 2000; Ubierna *et al.*, 2013):

$$V_c = \frac{A + R_D}{1 - \frac{\gamma^* O_{bs}}{C_{bs}}}$$

$$V_o = \frac{V_c - A - R_D}{0.5}$$

$$V_p = \frac{xJ_t}{2}$$

where $\gamma^\star$ is half the reciprocal of Rubisco specificity at 35 °C (0.000291) and x is the fraction of J_t allocated to the C_4 cycle, 0.4–40% of the total electron flux is used for the C_4 portion of the cycle (von Caemmerer, 2000; Ubierna *et al.*, 2011). O_{bs} and C_{bs} are the the partial pressure of oxygen and CO_2 in the bundle sheath cells, respectively:

$$O_{bs} = \frac{\alpha A}{0.047 g_{bs}} + O_m$$

$$C_{bs} = \frac{(\gamma^* O_{bs})(\frac{7}{3}(A + R_D) + \frac{(1-x)J_t}{3}}{\frac{(1-x)J_t}{3} - (A + R_D)}$$

where, g_{bs} is the bundle sheath conductance in sorghum (0.00113 mol m^{-2} s^{-1}; Brown and Byrd, 1993) and O_m is the oxygen partial pressure in the mesophyll cell, assumed to be equal to the partial pressure of oxygen in the intercellular airspace (mesophyll conductance is infinite). We modeled J_t, the total electron transport rate as a function of photosynthetic rate, using the equations for the light-limited C_4 photosynthesis model of von Caemmerer (2000):

$$J_t = \frac{-\mathrm{II} + \sqrt{\mathrm{II}^2 - 4 \times \mathrm{III} \times \mathrm{I}}}{2 \times \mathrm{III}}$$

where,

$$\mathrm{I} = \left(1 + \frac{R_D}{A}\right) \times \left(R_m - g_{bs} C_m - \frac{7 g_{bs} \times \gamma^* O_m}{3}\right) + (R_D + A) \times \left(1 - \frac{7\alpha\gamma^*}{3 \times 0.047}\right)$$

$$\mathrm{II} = \frac{1-x}{3}\left[\frac{g_{bs}}{A}\left(C_m - \frac{R_m}{g_{bs}} - \gamma^* O_m\right) - 1 - \frac{\alpha \times \gamma^*}{0.047}\right] - \frac{x}{2}\left(1 + \frac{R_D}{A}\right)$$

and

$$\mathrm{III} = \frac{x - x^2}{6A}$$

where α is the fraction of PSII activity in the bundle sheath (0 in sorghum).

Enzyme activity assays

Activities of three key C_4-specific photosynthetic enzymes, pyruvate orthophosphate dikinase (PPDK), PEPC, and malate dehydrogenase (MDH), were measured in crude extracts from sun and shade leaves collected from the Urbana site on 4 September 2017. Samples of ~60 mg each were collected, flash-frozen, and hand-ground under liquid nitrogen. Proteins were then extracted, following the protocol of Pittermann and Sage (2000), in a buffer of 50 mM HEPES (pH 8.2), 1% polyvinylpyrrolidone, 0.14% (w/v) BSA, 5 mM DTT, 10 mM $MgCl_2$, 10% (v/v) glycerol, 1 mM EDTA, and one protease inhibitor cocktail tablet per 50 ml of buffer, for 20 min at room temperature on a shaker. Extracts were centrifuged at full speed for 60 s and separated into aliquots for the analyses.

PPDK was assayed using the method of Pittermann and Sage (2000) with the modifications of Wang *et al.* (2008). Assay buffer was comprised of 50 mM Tris (pH = 7.7), 7 mM DTT, 4 mM glucose-6-phosphate, 10.5 U ml^{-1} porcine MDH, 1 U ml^{-1} microbial PEPC, 5 mM $MgCl_2$, 1.5 mM EDTA, 10 mM $NaHCO_3$, 5 mM NH_4Cl, 2.5 mM K_2HPO_4, 0.3 mM NADH, 2 mM ATP, and 1 U ml^{-1} myokinase. An aliquot of 20 µl of leaf extract was added to 270 µl of buffer and the reaction was initiated with addition of 30 µl of 20 mM sodium pyruvate.

MDH was assayed following a modification of Kumar *et al.* (2000). The reaction buffer comprised 100 mM Tris–HCl (pH = 7.8), 30 mM DTT, 0.5 mM EDTA, 0.3 mM NADPH, 8 mM $MgCl_2$, 10 mM $NaHCO_3$, 1 U ml^{-1} PEPC, and 2 mM glucose-6-phosphate. The reaction was initiated with addition of 30 µl of 20 mM PEP to a mixture of 20 µl of leaf extract and 270 µl of buffer, following incubation for 20 min to achieve activation of the enzyme.

PEPC was assayed following Sales *et al.* (2018). The assay buffer included 50 mM Tris–HCl (pH = 7.8), 5 mM $MgCl_2$, 10 mM $NaHCO_3$, 0.3 mM NADH, 10.5 U ml^{-1} porcine MDH, 1 mM EDTA, and 2 mM glucose-6-phosphate. An aliquot of 20 µl of leaf extract was added to 270 µl of buffer and the reaction was initiated with addition of 30 µl of 20 mM pyruvate. In all three assays, the reaction rate was measured as change in absorbance of NADH or NADPH at 340 nm using an extinction coefficient of 6.22 M^{-1} cm^{-1}. Measurements were done at 30 °C. PEPC was assayed over the course of 10 min and extrapolated to t=0, using the observed exponential decrease in reaction rate with time, to account for end-product inhibition: the other two enzymes were assayed over the course of 10 min. All chemicals were from Sigma-Aldrich (St. Louis, MO, USA).

Since Rubisco was not measured in 2017 due to limited sample material, tissue samples from upper and lower canopy leaves of erectophile and planophile accessions were collected on 12 August 2020. Protein extractions were performed as described above. Rubisco content was assayed via a competitive ELISA, using the Plant Rubisco ELISA Kit (Aviva Systems Biology, San Diego, CA, USA). Protein extracts (50 µl) were incubated along with 50 µl of anti-Rubisco antibody solution, in well plates pre-coated with Rubisco, for 60 min at 37 °C. Wells were then washed and incubated with a secondary antibody conjugated to horseradish peroxidase (100 µl), for 60 min at 37 °C. Finally, wells were thoroughly washed again and incubated with 90 µl of tetramethylbenzidine solution for 20 min at 37 °C. Absorbance was read at 450 nm and compared with a standard curve.

Statistical analysis

Photosynthetic data were analyzed via two distinct methods. The first was an analysis of covariance, to explore whether canopy type (erectophile versus planophile) modulated the effect of canopy position, after controlling for height. The effects of year×site were combined to give an 'environment' term, so that there were a total of n=4 'environments'. Individual accessions were only replicated at two sites per year, and estimating effects of accessions would be difficult. Therefore, we omitted the effect of accession from our model, treating accessions as individual observations within the broader population of erectophile or planophile types, and analyzed data using plant height as a covariate:

$$y = \mu + \text{type} + \text{height} + \text{environment} + \text{type} \times \text{environment} + \text{position} + \text{type} \times \text{position}$$

Here, y represents each photosynthetic parameter, μ is the grand mean, 'type' represents erectophile or planophile canopy structure (two levels), 'height' represents plant height used as a covariate, 'environment' is the combined effect of year×type (four levels), 'position' represents high or low canopy position (two levels), and 'type×position' interaction (four levels) would indicate that that the degree of self-shading, as hypothesized, modulates the effect of canopy position.

Enzyme activity and leakiness data were collected at only a single site, in one year, thus effects of environment and accession could not be estimated. The model here, therefore, omitted the environment term and accession terms, and analyzed data as a split plot design with 'type' (erectophile versus planophile) and 'position' as the split plot factor. Height was not included in 2020 as height estimates had not been concluded at the time of submission. Failures in the harvester meant that not all accessions were harvested in each year at each site; therefore, data from both sites were combined. The model was the following, with 'year' representing the effect of calendar year.

$$y = \mu + \text{type} + \text{height} + \text{year}$$

Additionally, data were analyzed using a paired design, comparing upper and lower canopy leaves within each accession to estimate the effect of canopy position and the interaction of type×position. In the paired design, each accession was treated as a single individual, pooling across the two sites and across the two years, in cases where the accession was sampled in both years. The difference between values for upper and lower canopy leaves (Δy, e.g. $\Delta A_{sat}=A_{sat,upper}-A_{sat,lower}$) within each plot was used as the response variable. The Δy values for erectophile and planophile accessions were compared to estimate the effect of 'position × type', and the combined Δy values for both classes (erectophiles + planophiles) were compared against 0 to estimate the effect of 'position'. For 'position × type', a significant effect shows, as above, that the degree of self-shading modulates the effect of canopy position. In addition, since leaf angle could be considered as a continuous rather than a categorical variable, each variable was subjected to linear regression against leaf angle, treating each accession as a data point. Linear regression was done separately for 2016 and 2017.

Homogeneity of variance was assessed by Hartley's test. To improve homogeneity of variance for ANOVA and planned contrasts, values for electron transport under ambient light conditions ($J_{ambient}$), assimilation rate under ambient conditions ($A_{ambient}$), the ratio of electron transport quantum yield to assimilation quantum yield (Φ_J/Φ_{CO2}), intrinsic water use efficiency at ambient light ($IWUE_{ambient}$), and stomatal conductance at saturating light ($g_{S,sat}$) were cube-root transformed. For the same reason, quantum yield of electron transport (Φ_J), PEPC activity, PPDK activity, and incident light (Q) were square-root transformed. All statistical analyses used the ANOVA procedure in STATA 15.1 (Stata Statistical Software: Release 15 StataCorp LLC, College Station, TX, USA).

Results

Screening for leaf angle and effects on light transmission in diverse accessions

The biodiversity panel showed large variation in leaf inclination angle. Leaf angles for the youngest fully expanded leaf averaged 9–12° in 'erectophiles' and 44–48° for 'planophiles' in 2016, and 10–12° and 44–49°, respectively, in 2017. Distributions of leaf angles are shown in Fig. 1, with combined data from 2016 and 2017. Leaf erectness in all 4 years of the study had a profound impact on light penetration through the canopy. Averaged across the 4 years of measurements, the lowermost fully green leaf of erectophiles received 175% more light than in planophiles (Table 1). Extinction coefficients were 2.26 in erectophiles versus 3.15 in planophiles in July 2018 (t=2.32, P=0.029, df=24), 3.37 versus 4.42 in August 2018 (t=4.10, P<0.001, df=16: Fig. 2), and 2.60 versus 3.60 in July 2020 (t=2.32, P=0.029, df=24). The generally higher extinction coefficients in August compared with July 2018 reflect the taller and denser canopy structure achieved by this growth stage. Leaf angles for the accessions in 2016 and 2017 are given in Supplementary Tables S1 and S2, respectively. Parameters extracted from light profiles in 2018 are given in Supplementary Table S3, while light profiles measured in 2020 are given in Supplementary Table S4.

Leaf absorptance was, as expected, strongly affected by canopy position. Lower canopy leaves had significantly higher leaf absorptance than upper canopy leaves: this effect was larger in planophiles (4% increase, from 0.831–0.865 to 0.869–0.909) than in erectophiles (2% increase, from 0.832–0.847 to 0.845–0.870). Plant height did not vary between canopy types, averaging 365 cm in 2016 and 331 cm in 2017.

Carbon assimilation

Consistent with our hypothesis, the reduction in quantum yield of carbon assimilation ($\Phi_{CO2,max,abs}$) in the lower canopy was greater in planophile than in erectophile accessions across the two years ($F_{12,143}$=4.08, P=0.013: Fig. 3). In 2016, among the planophile accessions, $\Phi_{CO2,max,abs}$ dropped to 0.025–0.038 in the lower canopy, compared with 0.054–0.070 in the upper canopy (a 47% decrease), whereas, in the erectophile accessions, $\Phi_{CO2,max,abs}$ only decreased to 0.041–0.054 in the lower canopy, representing a 26% decrease

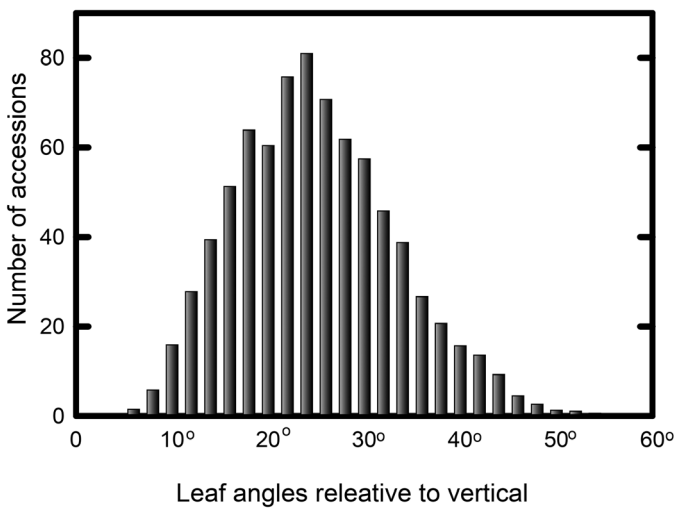

Fig. 1. Measurement of the leaf inclination angle. Leaf inclination angle (relative to the vertical) for the youngest fully expanded leaf of 869 sorghum accessions, measured in July 2016 and July 2017 at two sites (Savoy, IL and Urbana, IL).

Table 1. Means (±SE), r^2 for correlation against leaf inclination angle, Student's *t*-values for planned contrasts, and *F*-values from ANOVA, for maximal light-saturated carbon assimilation (A_{sat}), light-adapted respiration (R_D), convexity of the light–response curve (θ), incident photosynthetically active radiation (*Q*), light-saturated stomatal conductance ($G_{S,sat}$), water use efficiency at ambient light level in the field ($IWUE_{ambient}$), and slope of the stomatal conductance versus light–response curve (Φ_G), for sun leaves and shaded leaves of erectophile (E) and planophile (P) sorghum accessions

Variable:	A_{sat}	R_D	Θ_A	*Q*	$g_{S,sat}$	$IWUE_{ambient}$	Φ_g
Treatment	**μmol m^{-2} s^{-1}**		**–**	**μmol m^{-2} s^{-1}**	**mol m^{-2} s^{-1}**	**μmol mol^{-1}**	**mol mmol^{-1}**
P, Sun (2016)	30.1±2.6	1.5±0.1	0.56±0.05	1949±49	0.149±0.014	162±11	02.54±2.6
P, Shade (2016)	13.3± 1.5	0.9±0.1	0.54±0.03	108±12	0.061±0.010	62±7	1.68±1.6
Reduction (%)	56	40	4	94	58	61	34
E, Sun (2016)	27.7±2.0	1.6±0.1	0.66±0.05	1661±86*	0.139±0.005	166±7	3.46± 6.9
E, Shade (2016)	15.6±1.4	1.1±0.2	0.52±0.03	300±29***	0.065±0.009	160±33***	4.36±1.39
Reduction (%)	43	33	23	82	52	4	–26
P, Sun (2017)	37.8±3.3	2.4±0.3	0.46±0.05	1690±29	0.168±0.018	189±8	2.00±1.6
P, Shade (2017)	19.6±1.8	1.2±0.2	0.40±0.07	165±32	0.080±0.011	158±18	1.70±3.0
Reduction (%)	48	51	12	90	52	16	16
E, Sun (2017)	35.1±2.0	2.1±0.1	0.50±0.05	1674±24	0.146±0.009	185±5	2.15±1.1
E, Shade (2017)	23.9±1.5	1.7±0.1*	0.36±0.04	324±39**	0.104±0.009	179±12	1.87±1.7
Reduction (%)	32	18	28	81	28	3	13
Correlation							
2016	0.010	0.072	0.122	0.675**	0.006	0.184	0.198
2017	0.170	0.188*	0.002	0.237*	0.150	0.056	0.027
Contrast							
Position	–9.74***	–6.73***	–2.85*	–27.45***	–8.40***	–3.70***	0.84
Type× Position	–2.20*	–2.45*	1.65	–5.26***	–1.44	–3.21**	–1.44
Source of variation							
	$F_{12,143}$	$F_{12,143}$	$F_{12,143}$	$F_{12,143}$	$F_{12,143}$	$F_{12,143}$	$F_{12,143}$
Environment	5.07**	4.91**	21.72***	0.93	0.51	0.61	2.13
Type	0.01	2.25	0.37	24.89***	0.27	13.28***	6.58*
Height	1.25	0.23	0.39	4.29*	0.09	1.37	0.55
Env×type	0.07	0.85	0.15	3.02*	1.17	1.50	0.65
Position	48.29***	21.69***	3.00	1905.20***	43.77***	19.71***	0.18
Type×Position	2.07	3.81*	1.03	42.14***	2.02	8.58***	1.36

$IWUE_{ambient}$ was estimated at ambient light levels for each leaf at midday on a fully sunlit day in August; A_{sat} and $G_{S,max}$ were measured under light-saturated conditions, while Φ_G was measured under light-limited conditions (PAR=0–150 μmol m^{-2} s^{-1}). Eight planophile and 10 erectophile lines were measured in 2016; nine planophile and 12 erectophiles were measured in 2017. Correlation (r^2) refers to the correlation of parameter values for lower canopy leaves against leaf angle, since changes in light distribution are expected to have the strongest effects in the lower canopy. Data are from a pair of field studies in 2016 and 2017 (Savoy, IL and Urbana, IL). In both years, each accession was replicated at two field sites. Symbols '*', '**', and '***' denote statistical significance at a two-tailed probability; α=0.05, 0.01, and 0.001, respectively. This is for comparison of both erectophiles with planophiles at the same canopy position and within the same year, and for correlation, contrast, and sources of variation.

(*t*=4.14, *P*=0.0012, df=13 for the type×position contrast). Similar effects were evident in 2017: in planophile accessions, $\Phi_{CO2,max,abs}$ was 30% lower in lower canopy leaves than in the upper canopy, while the corresponding decrease was only 12% in erectophiles (*t*=2.25, *P*=0.037, df=18 for the type×position contrast). When the leaf inclination angle was considered as a continuous variable, lower canopy quantum yield was negatively correlated with inclination angle in both 2016 (r^2=0.72, *P*=0.0008) and 2017 (r^2=0.30, *P*=0.0101). Light-adapted respiration, like quantum yield, also showed evidence of a decrease in the lower canopy that was modulated by shade intensity. In 2017, R_D in lower canopy leaves was 18% lower than for upper canopy leaves in erectophiles, but 52% lower in planophiles (*t*=2.31, *P*=0.033, df=7). Statistical analyses for $\Phi_{CO2,max,abs}$ and $\Phi_{CO2,max,app}$ results are given in Supplementary Table S5. Parameters extracted from light–response curves are presented in Supplementary Tables S6 and S7 for 2016 and 2017, respectively. Raw data from light–response curves are shown in Supplementary Tables S8 and S9 for 2016 and 2017, respectively.

In both years, light-saturated photosynthetic capacity (A_{sat}) was much lower in the lower canopy. For example, in 2016, lower canopy rates were 12–21 μmol m^{-2} s^{-1}, compared with 25–35 μmol m^{-2} s^{-1} in the upper canopy. As with respiration and quantum yield, this effect was less pronounced in erectophiles, with a 34% reduction versus 50% in planophiles (Table 1). The effect of shade intensity on modulating the effect of canopy position was therefore smaller for A_{sat} than for quantum yield. Although the convexity of the *A* versus *Q* light–response curve was significantly lower in the lower

canopy, the difference between erectophiles and planophiles was not significant (Table 1).

Because of the compounding effect of greater light availability, higher A_{sat} and higher $\Phi_{CO2,max,app}$, with a small offset from higher R_D, lower canopy leaves of erectophile lines have substantially higher estimated carbon assimilation at midday on sunny days in mid-summer ($A_{ambient}$: $F_{12,143}$=18.81, P<0.0001). Based on field measurements of light availability in the upper and lower canopy, lower canopy leaves of erectophiles supported 3.2-fold greater carbon assimilation than lower canopy leaves in planophiles in 2016 (4.4–7.8 μmol m^{-2} s^{-1} versus 0.9–2.9 μmol m^{-2} s^{-1}: t=6.38, P=0.0011, df=15: Fig. 4) and 72% more assimilation in 2017 (6.7–11.2 μmol m^{-2} s^{-1} versus 3.1–11.3 μmol m^{-2} s^{-1}: t=3.25, P=0.0047, df=17; Fig. 4). Considering leaf inclination angle as a continuous variable, lower canopy estimated carbon assimilation ($A_{ambient}$) was negatively correlated with leaf angle in both 2016 (r^2=0.652, P<0.0001: Fig. 5) and 2017 (r^2=0.343, P=0.586: Fig. 6). There was no significant difference in upper canopy assimilation between erectophiles and planophiles: therefore, expected levels of overall canopy-level photosynthesis would be higher in the erectophile accessions.

To quantify the whole-canopy difference in assimilation, we plotted each photosynthetic parameter (α, $\Phi_{CO2,max,abs}$, R_D, and A_{sat}) as a function of ambient light for (i) upper canopy leaves of both types; (iii) lower canopy leaves of erectophiles; and (iii) lower canopy leaves of planophiles. From these three points, we estimated linear relationships for each variable (A_{sat}=0.0096Q + 16.04, R_D=0.0017Q+0.843, $\Phi_{CO2,max,app}$=0.0001Q + 0.0399). θ was set at 0.5, since no position×type effect was detected (Table 1). The ambient light environment through the canopy was predicted (in increments of 0.01 of canopy depth) from the measured light extinction coefficients for July and August, assuming that leaves were evenly distributed through the canopy and that overall canopy LAI was 5.0, and these 100 increments were summed to obtain estimated whole-canopy

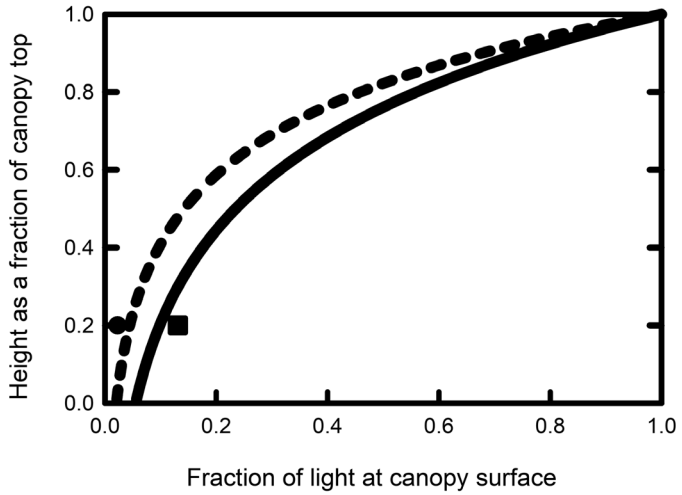

Fig. 2. Fraction of incident light retained. Fraction of incident light (relative to full sunlight) retained, as a function of relative height from the top of the canopy to the ground (1.0=top of canopy, 0=ground surface) in sorghum accessions with small leaf inclination angles from the vertical (erectophile: solid line) and large leaf inclination angles (planophile: broken line). Light profiles were measured with a line quantum sensor in July and August 2018, averaged across the accession selected for photosynthesis measurements. In addition, light at one-fifth of the canopy height, approximating to the lowest fully green leaves, was measured in each year. The fraction of light remaining at this height averaged across the lines used for photosynthesis, for both study sites in July and August of each of 2016, 2017, and 2018, is given for the planophile (filled circle) and erectophile (filled square) accessions.

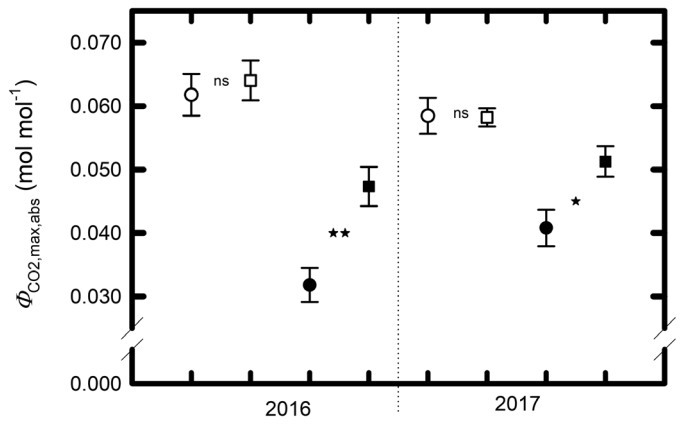

Fig. 3. Mean maximum quantum yields of leaf CO_2 uptake. Mean maximum quantum yields (±1 SE) of leaf CO_2 uptake on an absorbed light basis ($\Phi_{CO2,max,abs}$) in sun leaves (open symbols) and shade leaves (filled symbols) of planophile and erectophile sorghum accessions, respectively. Means are based on eight planophile and 10 erectophile accessions in 2016, and nine planophile and 12 erectophile accessions in 2017, respectively. Symbols '*' and '**' represent statistical significance at α=0.05 and 0.01, respectively, when comparisons are made between erectophiles and planophiles at the same canopy position within the same year (ns, α>0.05). Data are from both field sites.

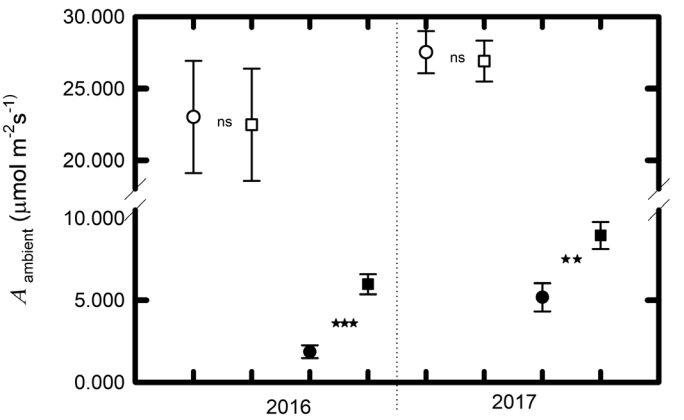

Fig. 4. Mean maximum quantum yields of leaf CO_2 uptake on an absorbed light basis. Mean leaf CO_2 uptake ($A_{ambient}$±1 SE) at the ambient light level in the field in sun leaves (open symbols) and shade leaves (filled symbols) of planophile and erectophile sorghum accessions, respectively. Means are for the same leaves as sampled in Fig. 3. Symbols '**' and '***' represent statistical significance at α=0.01 and 0.001, respectively, when comparisons are made between erectophiles and planophiles at the same canopy position within the same year (ns, α>0.05). Data are from both field sites.

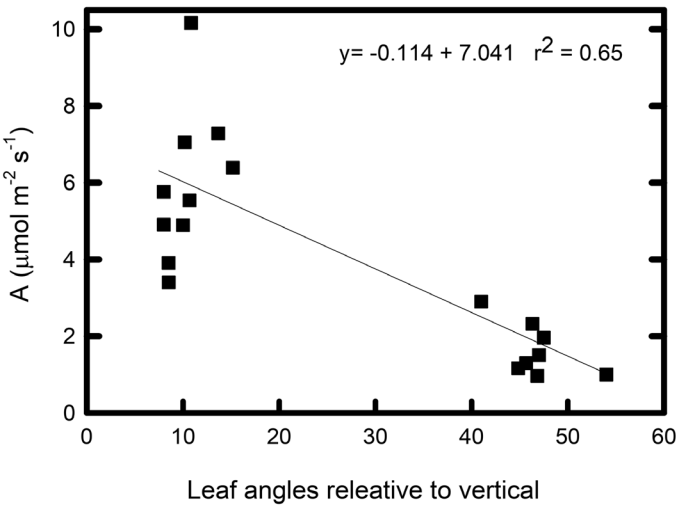

Fig. 5. Carbon assimilation at ambient light level in 2016. Estimated carbon assimilation at ambient light level in the field ($A_{ambient}$) as a function of leaf inclination angle (relative to the vertical) across 18 sorghum accessions; 10 erectophiles and eight planophiles for both field sites in 2016.

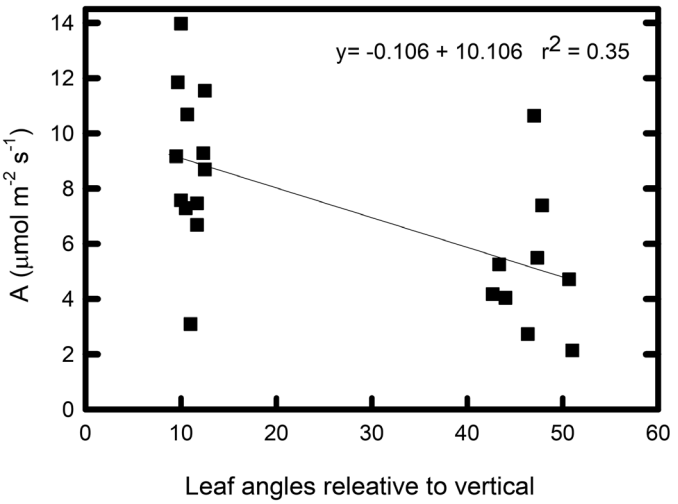

Fig. 6. Carbon assimilation at ambient light level in 2017. Estimated carbon assimilation at ambient light level in the field ($A_{ambient}$) as a function of leaf inclination angle (relative to the vertical) across 21 sorghum accessions; 12 erectophiles and nine planophiles for both field sites in 2017.

photosynthesis (calculations shown in Supplementary Table S10). By counterfactually changing only the extinction coefficient and absorptance, and not changing the photosynthetic parameters (i.e. assuming no shade-related decline in leaf photosynthetic traits), the share of the decline in lower canopy assimilation due to the direct effect of less light in the lower canopy was projected. This allowed separation of any additional change due to the greater decline in $\Phi_{CO2,max,abs}$, R_D, and A_{sat} in the planophile canopies. Based on these assumptions, planophile canopies would have 19% lower photosynthesis in July, with 83% of this decline due to direct effects of less light in the lower canopy and 17% due to the greater decline in photosynthetic capacity. In August, under heavier self-shading, the projected decline in planophiles relative to erectophiles was 21%, of which 89% was due to less light and 11% due to greater loss of photosynthetic capacity. In early season growth (June), self-shading would be less in both canopy types. Although measurements were not made in June, losses were projected assuming the same light-dependent changes observed in July and August. With assumed extinction coefficients of k=0.8 and 1.8 in erectophile and planophile canopies, respectively, planophiles would show 22% lower whole-canopy photosynthesis, with 64% of the decrease being due to lower light availability and 36% due to a greater decline in photosynthetic traits. This suggests that the greater loss of photosynthetic capacity in planophile canopies might have most impact in early season growth, but would be substantial throughout. A linear decline in assimilation from low to high leaf angle is presented (Figs 5, 6). However, our selection of the extremes in canopy types from the original results in two clusters, leaves some uncertainty in the assumption of linearity which would affect the calculated losses, but not their direction. Results of the full statistical analysis for $A_{ambient}$ are in given in Supplementary Table S10, including erectophiles, planophiles, and counterfactual scenarios where only light environment or only photosynthetic traits, respectively, are changed. Light–response curves for upper and lower canopy leaves in 2016 and 2017 are shown graphically in Supplementary Figs S1–S4.

Electron transport

The response of whole-chain electron transport to light (J versus Q) in both years showed less depression of quantum yield in the lower canopy than the A versus Q responses, and no significant difference between erectophiles and planophiles (Table 2). For example, in 2017, Φ_J in lower canopy leaves was 12–15% lower than in upper canopy leaves; this was equivalent to the modest decrease in $\Phi_{CO2,abs}$ in erectophile lower canopy leaves, and only half as large as the 30% decrease in the planophiles. The comparison of changes for electron transport and assimilation might indicate decoupling of electron transport and net CO_2 assimilation under low light. Pooling across both years, the $\Phi_J/\Phi_{CO2,abs}$ ratio increased from 5.3–5.5 in the upper canopy to 6.0–6.3 in erectophile lower canopy leaves (t=2.51, P=0.023, df=17), but from 5.4–5.6 to 8.5–9.3 in planophiles (t=5.42, P<0.0001, df=16). This ratio is an index of how much reducing power is required to assimilate a molecule of CO_2: therefore, such decoupling could potentially be linked to greater bundle sheath leakiness at low light or diversion of reductive power to sinks other than CO_2 assimilation

Maximal electron transport capacity (J_{sat}) was higher in sun leaves than in shade leaves (132–161 µmol m^{-2} s^{-1} versus

Table 2. Means (±SE), Student's *t*-values for planned contrasts, r^2 values for correlation against leaf inclination angle, and *F*-values for quantum yield of electron transport under light-limited conditions (Φ_J), maximal potential PSII efficiency at saturating light (F_V'/F_M'), ratio of quantum yield of electron transport to quantum yield of carbon assimilation (Φ_J/Φ_{CO2}), electron transport at ambient light levels ($J_{ambient}$), and light-saturated electron transport rate (J_{sat}) for sun leaves and shaded leaves of a set of erectophile (E) and planophile (P) sorghum accessions

Treatment	Φ_J	F_V'/F_M'	Φ_J/Φ_{CO2}	$J_{ambient}$	J_{sat}
	mol electrons mol^{-1} light		–	µmol m^{-2} s^{-1}	µmol m^{-2} s^{-1}
P, Sun (2016)	0.358±0.008	0.337±0.007	5.98±0.18	121.3±16.2	134.7±20.1
P, Shade (2016)	0.329±0.027	0.308±0.014	11.88±0.93	29.0±3.1	127.2±16.0
Reduction (%)	8	8	–99	76	6
E, Sun (2016)	0.340±0.010	0.328±0.008	5.60±0.32	120.9±9.6	137.9±12.4
E, Shade (2016)	0.308±0.011	0.297±0.011	7.05±0.48***	56.9±4.3 ***	118.2±12.1
Reduction (%)	9	9	–26	53	14
P, Sun (2017)	0.294±0.009	0.303±0.010	5.09±0.14	171.9±10.0	202.6±17.4
P, Shade (2017)	0.251±0.017	0.266±0.021	6.20±0.24	31.7±4.9	115.0±12.4
Reduction (%)	15	12	-22	82	43
E, Sun (2017)	0.292±0.005	0.304±0.009	5.13±0.12	169.7±6.0	200.4±10.0
E, Shade (2017)	0.258±0.008	0.296±0.008	5.40±0.25*	60.4±6.6 **	147.0±10.9
Reduction (%)	12	3	–5	64	35
Correlation					
2016	0.001	0.000	0.652***	0.636***	0.031
2017	0.000	0.091	0.265*	0.348**	0.168
Position	–4.23***	–3.85**	5.11***	–13.48***	4.13***
Type×Position	–0.13	–0.99	–3.59**	–3.49**	–0.32
Source of variation					
	$F_{12,143}$	$F_{12,143}$	$F_{12,143}$	$F_{12,143}$	$F_{12,143}$
Environment	9.03***	2.24	2.13	10.92***	7.15***
Type	0.86	0.16	24.93***	15.61***	0.21
Height	4.42*	0.02	1.01	2.80	0.35
Env×Type	1.79	0.60	0.41	0.17	0.08
Position	11.04***	5.84**	35.36***	162.99***	12.03***
Type×Position	0.17	0.94	13.01***	8.40***	0.76

$J_{ambient}$ was measured at ambient light levels for each leaf, at midday on a clear sky day in August; Φ_J and Φ_J/Φ_{CO2} were measured over the light-limited range of photosynthesis (0–150 µmol m^{-2} s^{-1}), and F_V'/F_M' and J_{max} were measured at saturating light. Samples and statistical symbols are as in Table 1.

83–111 µmol m^{-2} s^{-1}), but there were no differences between erectophiles or planophiles in either J_{sat} or the response of J_{sat} to canopy position (i.e. no interaction between canopy position and canopy type: Table 2). The convexity of the electron transport versus light curve (θ_J) was unaffected by light (Supplementary Table S3). As noted for gas exchange, electron transport-related parameters extracted from light–response curves are presented in Supplementary Tables S6 and S7 for 2016 and 2017, respectively, while raw data are shown in Supplementary Tables S8 and S9 for 2016 and 2017, respectively.

Water use efficiency

Neither the initial slope nor the convexity of the stomatal conductance versus light curve was affected by canopy position or canopy structure (Table 1). Light-saturated maximal conductance ($g_{S,sat}$) was higher in upper canopy leaves than in lower canopy leaves. However, this effect of canopy position was similar in planophiles and erectophiles. The combination of higher assimilation and similar stomatal conductance, in lower canopy leaves of erectophiles compared with planophiles, resulted in a large advantage for erectophiles in $IWUE_{ambient}$ (Table 1). While upper canopy leaves of both forms had similar intrinsic water use efficiency, $IWUE_{ambient}$ was >50% higher in lower canopy leaves of erectophiles compared with planophiles (168–188 µmol mol^{-1} versus 105–121 µmol mol^{-1}: t=3.89, P=0.002, df=13).

Bundle sheath leakiness

Bundle sheath leakiness, among the 12 accessions surveyed in summer 2020, showed no change with descending canopy position, when measured either at high or at low irradiance (Table 3). Consistent with previous findings (e.g. Kromdijk *et al.*, 2008), leakiness was much higher at low irradiance: when each leaf was measured at 2200 µmol m^{-2} s^{-1} and at 80 µmol m^{-2} s^{-1}, ϕ at low light intensity was consistently higher (0.39–0.46 versus 0.27–0.31).

Productivity

Across 2016 and 2017, biomass was affected by height ($F_{1,35}$=9.68, P=0.004), by canopy type ($F_{1,35}$=23.58, P<0.001), and by sampling year ($F_{1,35}$=36.16, P<0.001). Erectophile accessions produced 33% more biomass than planophiles—a 6.5 Mg ha^{-1} difference (25.55±1.26 Mg ha^{-1} versus 19.07±1.47 Mg ha^{-1}: t=2.53, P=0.017, df=31). Effects of leaf erectness on productivity were also present when leaf angle was considered as a continuous rather than a categorical variable: leaf angle was also negatively correlated with biomass in both 2016 (r^2=0.37, P=0.0036) and 2017 (r^2=0.39, P=0.0026). Biomass data are shown in (Supplementary Tables S11 and S12 for 2016 and 2017, respectively.

C_4 photosynthetic enzymes

In 2017, all three of the C_4 cycle enzymes assayed showed clear trends, of comparable magnitude, towards lower activity in shade leaves; however, there was no evidence of differing shade responses in erectophile and planophile accessions (Table 4; (Supplementary Table S13). Maximal extractable PPDK activity in the 2017 samples was 30% lower in shade leaves than in sun leaves, while the V_{max} of PEPC was 36% lower and that of MDH was 39% lower.

In contrast to the C_4 cycle enzymes, the samples collected in 2020 showed no trend towards lower Rubisco content in the shade, or any difference between erectophiles and planophiles (Table 4; Supplementary Table S14).

Discussion

As hypothesized, our data indicate that the maximum quantum efficiency of CO_2 uptake ($\Phi_{CO2,abs}$), the key measure of photosynthetic efficiency in limiting light, declined in a maladaptive way into the lower canopy across 35 accessions of *S. bicolor*. However, the decline was much greater in planophile canopies, where the lowest fully green leaves received 5–10% of full sunlight, than in erectophile canopies, where the lowest corresponding leaves received 15–24% of full sunlight (Table 1; Fig. 2). The agronomic significance of the inability to acclimate to very low light environments is implicit in our study. Increasing leaf angles in cereals, including sorghum, has been associated with increased yields (Sinclair and Sheehy, 1999; Lee and Tollenaar, 2007; DaSilva and DeCosta, 2012; Lauer *et al.*, 2012; Richards *et al.*, 2019). This is largely because upper leaves in planophile canopies intercept more light than can be utilized in photosynthesis, while photosynthesis in the lower leaves is strongly light limited: erectophile forms therefore allow a more effective distribution of light. Here, in the case of sorghum,

Table 3. Means (±SE), r^2 values for correlation against leaf inclination angle, Student's t-values for planned contrasts, and F-values for carbon assimilation (A), stomatal conductance (g_S), and bundle sheath leakiness (ϕ), measured at two levels of light (2200 µmol m^{-2} s^{-1} and 80 µmol m^{-2} s^{-1}) in sun leaves and shaded leaves of a set of six erectophile (E) and six planophile (P) sorghum accessions

Treatment	***A***	***g*$_S$**	**ϕ**	***A***	***g*$_S$**	**ϕ**
	µmol m^{-2} s^{-1}	**mol m^{-2} s^{-1}**	**–**	**µmol m^{-2} s^{-1}**	**mol m^{-2} s^{-1}**	**–**
Photon flux:	**High**	**High**	**High**	**Low**	**Low**	**Low**
P, Sun	38.40±2.38	0.235±0.014	0.267±0.013	1.69±0.20	0.036±0.011	0.386±0.016
P, Shade	26.95±3.46	0.160±0.022	0.314±0.011	2.04±0.10	0.058±0.037	0.467±0.028
Reduction (%)	30	32	–18	–20	–54	–21
E, Sun	36.91±1.76	0.260±0.028	0.270±0.011	1.38±0.22	0.081±0.035	0.438±0.050
E, Shade	22.90±3.29	0.162±0.038	0.302±0.018	1.44±0.18	0.020±0.004	0.431±0.038
Reduction (%)	38	38	-12	-4	75	2
Correlation						
Upper canopy	0.029	0.001	0.000	0.006	0.001	0.001
Lower canopy	0.128	0.000	0.000	0.016	0.094	0.001
Contrast						
Level	–3.04**	–3.04*	1.79	0.96	–0.49	0.62
Type×Position	0.42	0.54	–0.47	–0.96	1.46	–1.06
Source of variation						
	$F_{14,9}$	$F_{14,9}$	$F_{14,9}$	$F_{14,9}$	$F_{14,9}$	$F_{14,9}$
Type	0.01	1.07	0.59	4.51	1.78	0.41
Position	9.19*	11.26**	2.83	8.50*	4.18	0.18
Type×Position	0.26	0.16	0.00	5.84*	1.30	0.35

Correlation (r^2) values refer to the correlation of parameter values against leaf angle, for both upper and lower canopy leaves. Data are from a summer 2020 field study in Urbana, IL. For cell means, symbols '*', '**', and '***' denote statistical significance at a two-tailed α=0.05, 0.01, and 0.001, respectively, when erectophiles are compared against planophiles at the same canopy position and within the same year. For F-values, r^2 values, and planned contrasts, symbols '*', '**', and '***' denote statistically significant effects of an explanatory variable at a two-tailed probability α=0.05, 0.01, and 0.001 respectively.

Table 4. Means (±SE) and *F*-values for maximal *in vitro* extractable activity (V_{max}) of pyruvate orthophosphate dikinase (PPDK), phosphoenolpyruvate carboxylase (PEPC), and NADP-dependent malate dehydrogenase (MDH), as well as Rubisco content, in sun leaves and shaded leaves of a set of erectophile accessions (small leaf inclination angle relative to vertical and low self-shading, denoted 'E') and planophile accessions (large leaf inclination angle relative to vertical and high self-shading, denoted 'P') of *Sorghum bicolor*

Treatment×Shade	PPDK	PEPC	MDH	Rubisco
	µmol m^{-2} s^{-1}	µmol m^{-2} s^{-1}	µmol m^{-2} s^{-1}	µg mg^{-1}
P, Sun	49.3±9.4	453.2±67.4	104.4±11.1*	2.45±0.31
P, Shade	37.4±4.1	304.8±49.7	56.7±14.8	2.35±0.20
Reduction (%)	24	33	46	22
E, Sun	50.0±6.4	418.7±61.6	70.9±17.8	2.57±0.17
E, Shade	33.2±4.5	263.3±22.0	45.4±14.0	2.30±0.22
Reduction (%)	34	37	36	80
Position	–2.79*	–2.97*	3.09*	0.69
Type×Position	0.71	-0.04	–0.96	0.33
Source of variation				
	$F_{21,13}$	$F_{21,13}$	$F_{21,13}$	
Type	0.26	0.35	0.00	0.14
Height	0.89	0.60	0.27	–
Position	10.38**	9.69**	10.87**	0.05
Type×Position	0.04	0.04	1.21	0.58

Activity data for PPDK, PEPC, and MDH were based on samples collected in early September 2017 (11 erectophile and nine planophile accessions): content data for Rubisco were based on samples collected in mid-August 2020 (12 erectophile and 12 planophile accessions). MDH was assayed after incubation with a high concentration of DTT to fully activate the enzyme. Activity measurements were done at 30 °C. For cell means, symbols '*', '**', and '***' denote statistical significance at a two-tailed α=0.05, 0.01, and 0.001, respectively, when erectophiles are compared against planophiles at the same canopy position, For *F*-values, symbols '*', '**', and '***' denote statistically significant effects of an explanatory variable at a two-tailed α=0.05, 0.01, and 0.001, respectively. Data for MDH, PEPC, and PPDK are from a 2016–2020 field study (Urbana, IL).

and possibly other crops of the Andropogoneae (Pignon *et al.*, 2017; Collison *et al.*, 2020), we show a second beneficial effect: maintenance of light-limited photosynthetic capacity and water use efficiency in the lower canopy leaves (Fig. 2). The fact that C_4 enzymes accounting for a significant amount of leaf soluble nitrogen were at similar levels in the lower canopy of planophiles and erectophiles (Table 4) suggests that nitrogen use efficiency might also be a further benefit of erectophile canopies. Here, leaf angle was only measured at the point of insertion into the stem. Sorghum leaves bow and so the angle will show a progressively larger angle with distance from the stem. Our assumption was that a low leaf angle at the point of insertion would result in lower angles across the leaf. That light reaching the lowest leaves in the erectophile canopies was double that of the planophile canopies, as judged by the angle at the point of insertion, suggests there was no compensatory effect, namely those with small angles at the point of insertion showing greater bowing (Fig. 2).

By comparing a wide range of germplasm, our results indicate that declines in quantum efficiency of carbon assimilation under self-shading are a species-wide phenomenon in sorghum, not limited to one or a few genotypes. In addition, much of the previous literature on sun versus shade acclimation has considered leaves grown under continuous high versus low light. Our study is relatively unusual in that it documents effects on $\Phi_{CO2,max,app}$ when C_4 leaves that emerge in high-light conditions are progressively subjected to increasingly heavy shade, a situation relevant to many agricultural and grassland environments. Previous studies found that self-shading in lower canopy leaves of *Miscanthus* and maize led to declines in $\Phi_{CO2,max,app}$, contrasting sharply with some C_3 crops such as wheat (Kromdijk *et al.*, 2008; Pignon *et al.*, 2017; Collison *et al.*, 2020). However, these studies considered only single genotypes; our data extend these previous studies by showing that quantum yield declines are a broadly observed pattern in sorghum, and are related to the degree of self-shading. Given that this has now been observed in three species of Andropogoneae, it suggests that this maladaptive response might apply to the full tribe.

The decline in Φ_J with canopy depth was much smaller than for Φ_{CO2} and was not affected by the degree of self-shading. This may indicate that increases in oxidative stress, non-photochemical quenching, or inefficiencies in carbon assimilation, leading to decoupling between electron transport and assimilation, could be part of the explanation for the decline in quantum yield under shading. However, increases in bundle sheath leakiness (ϕ) appear not to be the explanation for changes in Φ_J/Φ_{CO2}, since canopy position did not affect ϕ when sun and shade leaves were compared at the same light intensity. The lack of shade-induced increase in ϕ was consistent with the fact that Rubisco content showed much less of a decrease (not statistically significant) in lower canopy leaves than the mesophyll cycle photosynthetic enzymes, indicating that Rubisco in the bundle sheath should be able to keep up with the influx of CO_2 from the mesophyll. Previous literature has shown that bundle sheath leakiness increases with canopy depth in giant *Miscanthus,* from 0.2–0.5 under high light to 0.8 at the lowest light levels (Kromdijk *et al.*, 2008), while similar effects on leakiness are seen in maize (Kromdijk *et al.*, 2010), *Amaranthus* (Tazoe *et al.*, 2008), and *Flaveria* (Pengelly *et al.*, 2010). However, these effects seem to be purely the result of lower ambient light, and not an acclimatory response. Bellasio and Griffiths (2014) grew young maize plants of a single cultivar in high light and low light in controlled-environment cabinets. In parallel with the results here, ϕ was almost doubled in low light compared with high light (cf. Table 3). However, Bellasio and Griffiths found a slightly lower ϕ in the plants grown in low light, at all measurement light intensities, suggesting some acclimation. Here a significant difference between leaves in low light and high light was not found across 12 accessions.

In contrast to quantum yield and respiration rates, erectophile accessions showed similar declines in activity of C_4 enzymes to the planophiles. Activities of PPDK and MDH can co-limit the light-saturated photosynthetic rate, and therefore a decrease in the activity of these enzymes in lower canopy leaves is consistent with the observed decline in A_{sat}. The observed decreases in activity of C_4 enzymes, in the lower canopy, are also consistent with previous studies of C_4 plants grown under continuous high or low light (Sonawane *et al.*, 2018). Unlike the declines in Φ_{CO2}, these changes are likely to be adaptive. Since these parameters influence the maximum light-saturated rate of photosynthesis, decreased levels of the C_4-specific enzymes and of light-saturated photosynthetic capacity would be advantageous, allowing resources to be relocated to the upper leaves.

Breeders have long recognized that in this highly productive group of C_4 crops (Andropogoneae) erect leaf angle phenotypes are associated with elevated grain yields (Lee and Tollenaar, 2007; DaSilva and DeCosta, 2012; Lauer *et al.*, 2012; Lofton *et al.*, 2012; Zhang *et al.*, 2014; Truong *et al.*, 2015). These effects have been attributed entirely to a more effective distribution of light in the canopy (Gitz *et al.*, 2015). Likewise, previous modeling work has predicted the effect of reducing leaf angle through selection or synthetic biology on sorghum productivity, but has typically assumed large changes in light interception coupled with unchanged leaf photosynthetic traits (Gitz *et al.*, 2015; Truong *et al.*, 2015). This study identifies a different mechanism by which the erectophile form gains an important advantage, and indicates that the advantage of erectophile canopies could be even greater than previous models have predicted. The decline in capacity to assimilate CO_2 in the low-light conditions of the lower crop canopy appears an underappreciated explanatory factor for previously documented observational data. While the erectophile form reduces this loss, it is still present. Here all accessions were planted at the same density. However, if more erect form cultivars are grown at higher densities, the loss in efficiency seen here would be exacerbated. Understanding the mechanism, such that it might be eliminated, would lead to greater yield gains, especially if trends toward increasing planting density continue.

Supplementary data

The following supplementary data are available at *JXB* online.

Table S1. Leaf angles for 869 sorghum accessions in summer 2016.

Table S2. Leaf angles for 869 sorghum accessions in summer 2017.

Table S3. Parameters extracted from light profiles in erectophile and planophile sorghum canopies in summer 2018.

Table S4. Photosynthetically active radiation as a function of depth through the canopy in erectophile and planophile sorghum accessions in summer 2020.

Table S5. Means, SEs, and *F*-values from ANOVA for quantum yield of carbon assimilation, estimated carbon assimilation under ambient light conditions, and convexity of the electron transport curve for erectophile and planophile sorghum canopies.

Table S6. Parameters extracted from photosynthetic light–response curves for upper and lower canopy leaves of erectophile and planophile sorghum accessions, collected in summer 2016.

Table S7. Parameters extracted from photosynthetic light–response curves for upper and lower canopy leaves of erectophile and planophile sorghum accessions, collected in summer 2017.

Table S8. Raw data for light–response curves collected in summer 2016.

Table S9. Raw data for light–response curves collected in summer 2017.

Table S10. Predicted carbon assimilation at various increments of depth through the canopy, in erectophile and planophile sorghum accessions, under various hypothetical scenarios assuming changes in light penetration, changes in leaf-level photosynthetic traits, or both.

Table S11. Height and biomass data for selected erectophile and planophile sorghum accessions in summer 2016.

Table S12. Height and biomass data for selected erectophile and planophile sorghum accessions in summer 2016.

Table S13. *In vitro* activity of PEP carboxylase, pyruvate phosphate dikinase, and malate dehydrogenase in upper and lower canopy leaves of erectophile and planophile sorghum accessions in summer 2017.

Table S14. Rubisco content in upper and lower canopy leaves from erectophile and planophile sorghum accessions in summer 2020.

Fig. S1. Carbon assimilation (A_{sat}) as a function of incident light (I), along with fitted curves, in upper and lower canopy leaves of 10 sorghum accessions with highly erect leaves (erectophile canopy structure) in a 2016 field experiment.

Fig. S2. Carbon assimilation (A_{sat}) as a function of incident light (I), along with fitted curves, in upper and lower canopy leaves of eight sorghum accessions with drooping leaves (planophile canopy structure) in a 2016 field experiment.

Fig. S3. Carbon assimilation (A_{sat}) as a function of incident light (I), along with fitted curves, in upper and lower canopy leaves of 12 sorghum accessions with highly erect leaves (erectophile canopy structure) in a 2017 field experiment.

Fig. S4. Carbon assimilation (A_{sat}) as a function of incident light (I), along with fitted curves, in upper and lower canopy leaves of nine sorghum accessions with drooping leaves (planophile canopy structure) in a 2017 field experiment.

Acknowledgements

Grace Clayton, Katherine Ross, Charles Pignon, Megan Bernacchi, and Emily Gibson provided lab and field assistance. Dr Ryan Boyd helped with the leakiness models. This work was funded by the Water Efficient Sorghum Technologies project (Advanced Research Projects Agency-Energy, U.S. Department of Energy, under award number

DE-AR0-000661) and by the DOE Center for Advanced Bioenergy and Bioproducts Innovation (U.S. Department of Energy, Office of Science, Office of Biological and Environmental Research under award number DE-SC0018420). Any opinions, findings, and conclusions or recommendations expressed in this publication are those of the author(s) and do not necessarily reflect the views of the U.S. Department of Energy. The findings and conclusions in this publication are those of the author(s) and should not be construed to represent any official USDA or U.S. Government determination or policy

Author contributions

NSJ and SPL: conceptualization; ADBL, CJB, NSJ, PJB, SBF, and SSS; methodology, investigation, data curation, and analysis; NSJ, SPL, and SSS: writing—original draft; ADBL, CJB, NSJ, PJB, SBF, SPL, and SSS review and editing.

Data availability

All original data that support the findings of this study are freely available through the Illinois Data Bank https://doi.org/10.13012/B2IDB-4580996_V1

References

Bellasio C, Griffiths H. 2014. Acclimation to low light by C_4 maize: implications for bundle sheath leakiness. Plant, Cell & Environment **37**, 1046–1058.

Beyschlag W, Barnes PW, Ryel R, Caldwell MM, Flint SD. 1990. Plant competition for light analyzed with a multispecies canopy model: II. Influence of photosynthetic characteristics on mixtures of wheat and wild oat. Oecologia **82**, 374–380.

Bowling DR, Sargent SD, Tanner BD, Ehleringer JR. 2003. Tunable diode laser absorption spectroscopy for stable isotope studies of ecosystem–atmosphere CO_2 exchange. Agricultural and Forest Metereology **118**, 1–19.

Brown RH, Byrd GT. 1993. Estimation of bundle sheath cell conductance in C_4 species and O_2 insensitivity of photosynthesis. Plant Physiology **103**, 1183–1188.

Collison RF, Raven EC, Pignon CP, Long SP. 2020. Light, not age, underlies the maladaptation of maize and Miscanthus photosynthesis to self-shading. Frontiers in Plant Science **11**, 783.

De Silva ALC, DeCosta WAJM. 2012. Growth and radiation use efficiency of sugarcane under irrigated and rain-fed conditions in Sri Lanka. Sugar Tech **14**, 247–254.

dos Santos JPR, Fernandes SB, McCoy S, Lozano R, Brown PJ, Leakey ADB, Buckler ES, Garcia AAF, Gore MA. 2020. Novel bayesian networks for genomic prediction of developmental traits in biomass sorghum. G3 **10**, 769–781.

Duvick DN. 2005. The contribution of breeding to yield advances in maize (*Zea mays* L.). Advances in Agronomy **86**, 83–145.

Edwards GE, Baker NR. 1993. Can CO_2 assimilation in maize leaves be predicted accurately from chlorophyll fluorescence analysis? Photosynthesis Research **37**, 89–102.

Evans J, Sharkey T, Berry J, Farquhar G. 1986. Carbon isotope discrimination measured concurrently with gas exchange to investigate CO_2 diffusion in leaves of higher plants. Functional Plant Biology **13**, 281–292.

Farquhar GD. 1983. On the nature of carbon isotope discrimination in C_4 species. Functional Plant Biology **10**, 205–226.

Farquhar GD, Cernusak LA. 2012. Ternary effects on the gas exchange of isotopologues of carbon dioxide. Plant, Cell & Environment **35**, 1221–1231.

Gitz DC, Xin Z, Baker JT, Lascano RT, Burke JJ. 2015. Canopy light interception of a conventional and an erect leafed sorghum. American Journal of Plant Sciences **6**, 2576–2884.

Henderson SA, von Caemerrer S, Farquhar GD. 1992. Short term measurements of carbon isotope discrimination in several C_4 species. Functional Plant Biology **19**, 263–285.

Hikosaka K, Terashima I. 1995. A model of the acclimation of photosynthesis in the leaves of C_3 plants to sun and shade with respect to nitrogen use. Plant, Cell & Environment **18**, 605–618.

Hunt JR, Hayman PT, Richards RA, Passioura JB. 2018. Opportunities to reduce heat damage in rain-fed wheat crops based on plant breeding and agronomic management. Field Crops Research **224**, 126–138.

Ishida A, Uemura A, Koike N, Matsumoto Y, Hoe AL. 1999. Interactive effects of leaf age and self-shading on leaf structure, photosynthetic capacity and chlorophyll fluorescence in the rain forest tree, *Dryobalanops aromatica*. Tree Physiology **19**, 741–747.

Jin J, Xiaobing L, Guanghui W, Herbert SJ. 2003. Some ecophysiological characteristics of R4–R5 stage in relation to soybean yield differing in maturities. Agricultural Sciences in China **3**, 425–434.

Kromdijk J, Griffiths H, Schepers HE. 2010. Can the progressive increase of C_4 bundle sheath leakiness at low PPFD be explained by incomplete suppression of photorespiration? Plant, Cell & Environment **33**, 1935–1948.

Kromdijk J, Schepers HE, Albanito F, Fitton N, Carroll F, Jones MB, Finnan J, Lanigan GJ, Griffiths H. 2008. Bundle sheath leakiness and light limitation during C_4 leaf and canopy CO_2 uptake. Plant Physiology **148**, 2144–2155.

Kumagai E, Hamaoka N, Araki T, Ueno O. 2014. Dorsoventral asymmetry of photosynthesis and photoinhibition in flag leaves of two rice cultivars that differ in nitrogen response and leaf angle. Physiologia Plantarum **151**, 533–543.

Kumar RG, Shah K, Dubey RS. 2000. Salinity induced behavioural changes in malate dehydrogenase and glutamate dehydrogenase activities in rice seedlings of differing salt tolerance. Plant Science **156**, 23–34.

Lambert R, Johnson R. 1978. Leaf angle, tassel morphology and the performance of maize hybrids. Crop Science **18**, 499–502.

Lanigan GJ, Betson N, Griffiths H, Seibt U. 2008. Carbon isotope fractionation during photorespiration and carboxylation in *Senecio*. Plant Physiology **148**, 2013–2020.

Lauer S, Hall BD, Mulaosmanovic E, Anderson SR, Nelson B, Smith S. 2012. Morphological changes in parental lines of Pioneer brand maize hybrids in the US central Corn Belt. Crop Science **52**, 1033–1043.

Lee EA, Tollenaar M. 2007. Physiological basis of successful breeding strategies for maize grain yield. Crop Science **47**, S202–S215.

Lofton J, Tubana BS, Kanke Y, Teboh J, Viator H, Dalen M. 2012. Estimating sugarcane yield potential using an in-season determination of normalized difference vegetation index. Sensors **12**, 7529–7547.

Long SP, Postl WF, Bolhár-Nordekampf HR. 1993. Quantum yields for uptake of carbon dioxide in C_3 vascular plants of contrasting habitats and taxonomic groupings. Planta **189**, 226–234.

Loriaux SD, Avenson TJ, Welles JM, McDermitt DK, Eckles RD, Riensche B, Genty B. 2013. Closing in on maximum yield of chlorophyll fluorescence using a single multiphase flash of sub-saturating intensity. Plant Cell and Environment **36**, 1755-1770.

Marchiori PER, Machado EC, Ribeiro RV. 2014. Photosynthetic limitations imposed by self-shading in field-grown sugarcane varieties. Field Crops Research **155**: 30–37.

Mooney HA, Gulmon SL. 1979. Environmental and evolutionary constraints on the photosynthetic characteristics of higher plants. In: Solbrig OT, Jain S, Johnson GB, Raven PH eds. Topics in plant population biology. New York: Columbia University Press, 316–337.

Pendleton JW, Smith GE, Winter SR, Johnston TJ. 1968. Field investigations of the relationships of leaf angle in corn (*Zea mays* L.) to grain yield and apparent photosynthesis. Agronomy Journal **60**, 422–424.

Pengelly JJ, Sirault XR, Tazoe Y, Evans JR, Furbank RT, von Caemmerer S. 2010. Growth of the C_4 dicot *Flaveria bidentis*: photosynthetic acclimation to low light through shifts in leaf anatomy and biochemistry. Journal of Experimental Botany **61**, 4109–4122.

Pignon CP, Jaiswal D, McGrath JM, Long SP. 2017. Loss of photosynthetic efficiency in the shade. An Achilles heel for the dense modern stands of our most productive C_4 crops? Journal of Experimental Botany **68**, 335–345.

Pitterman J, Sage RF. 2000. Photosynthetic performance at low temperature of *Bouteloua gracilis* Lag., a high-altitude C_4 grass from the Rocky Mountains, USA. Plant, Cell & Environment **23**, 811–823.

Rai KN, Murthy DS, Andrews DJ, Bramel-Cox PJ. 1999. Genetic enhancement of pearl millet and sorghum for the semi-arid tropics of Asia and Africa. Genome **42**, 617–628.

Richards RA, Cavanagh CR, Riffkin P. 2019. Selection for erect canopy architecture can increase yield and biomass in spring wheat. Field Crops Research **244**, 107649

Roeske CA, O'Leary MH. 1984. Carbon isotope effects on the enzyme-catalyzed carboxylation of ribulose bisphosphate. Biochemistry **23**, 6275–6284.

Sales CRG, Ribeiro RV, Hayashi AM, *et al*. 2018. Flexibility of C_4 decarboxylation and photosynthetic plasticity in sugarcane plants under shading. Environmental and Experimental Botany **149**, 34–42.

Sinclair TR, Sheehy JE. 1999. Erect leaves and photosynthesis in rice. Science **283**, 1455.

Sonawane BV, Sharwood RE, Whitney S, Ghannoum O. 2018. Shade compromises the photosynthetic efficiency of NADP-ME less than that of PEP-CK and NAD-ME C_4 grasses. Journal of Experimental Botany **69**, 3053–3068.

Srinivasan V, Kumar P, Long SP. 2017. Decreasing, not increasing, leaf area will raise crop yields under global atmospheric change. Global Change Biology **23**, 1626–1635.

Syvertsen JP. 1984. Light acclimation in citrus leaves. II. CO_2 assimilation and light, water and nitrogen use efficiency. Journal of the American Horticultural Society **109**, 812–817.

Tazoe Y, Hanba YT, Furumoto T, Noguchi K, Terashima I. 2008. Relationships between quantum yield for CO_2 assimilation, activity of key enzymes and CO_2 assimilation in *Amaranthus cruentus*, a C_4 dicot, grown in high or low light. Plant & Cell Physiology **49**, 19–29.

Tazoe Y, von Caemmerer S, Badger MR, Evans JR. 2009. Light and CO2 do not affect the mesophyll conductance to CO2 diffusion in wheat leaves. Journal of Experimental Botany **60**, 2291-2301.

Tian F, Bradbury PJ, Brown PJ, Hung H, Sun Q, Flint-Garcia S, Rocheford TR, McMullen MD, Holland JB, Buckler ES. 2011. Genome-wide association study of leaf architecture in the maize nested association mapping population. Nature Genetics **43**, 159–162.

Truong SK, McCormick RF, Rooney WL, Mullet JE. 2015. Harnessing genetic variation in leaf angle to increase productivity of *Sorghum bicolor*. Genetics **201**, 1229–1238.

Ubierna N, Gandin A, Boyd RA, Cousins AB. 2017. Temperature response of mesophyll conductance in three C_4 species calculated with two methods: ^{18}O discrimination and *in vitro* V_{pmax}. New Phytologist **214**, 66–80.

Ubierna N, Sun W, Cousins AB. 2011. The efficiency of C_4 photosynthesis under low light conditions: assumptions and calculations with CO_2 isotope discrimination. Journal of Experimental Botany **62**, 3119–3134.

Ubierna N, Sun W, Cousins AB. 2013. The efficiency of C_4 photosynthesis under low light conditions in *Zea mays*, *Miscanthus* × *giganteus* and *Flaveria bidentis*. Plant, Cell & Environment **36**, 365–381.

Valluru R, Gazave EE, Fernandes SB, *et al.* 2019. Deleterious mutation burden and its association with complex traits in sorghum (*Sorghum bicolor*). Genetics **211**, 1075–1087.

von Caemmerer S. 2000. Biochemical models of leaf photosynthesis. Collingwood, Australia: CSIRO Publishing.

von Caemmerer S, Farquhar GD. 1981. Some relationships between the biochemistry of photosynthesis and the gas exchange of leaves. Planta **153**, 376–387.

von Caemmerer S, Ghannoum O, Pengelly JJ, Cousins AB. 2014. Carbon isotope discrimination as a tool to explore C_4 photosynthesis. Journal of Experimental Botany **65**, 3459–3470.

Wang D, Portis AR Jr, Moose SP, Long SP. 2008. Cool C_4 photosynthesis: pyruvate Pi dikinase expression and activity corresponds to the exceptional cold tolerance of carbon assimilation in *Miscanthus x giganteus*. Plant Physiology **148**, 557–567.

Williams WA, Loomis RS, Duncan WG, Dovrat A, Nunez F. 1968. Canopy architecture at various population densities and growth and grain yield of corn. Crop Science **8**, 303-8.

Wingate L, Seibt U, Moncrieff JB, Jarvis PG, Lloyd J. 2007. Variations in ^{13}C discrimination during CO_2 exchange by *Picea stichensis* branches in the field. Plant, Cell & Environment **30**, 600–616.

Xin Z, Gitz D, Burow G, Hayes C, Burke J. 2015. Registration of two allelic erect leaf mutants of sorghum. Journal of Plant Registrations **9**, 254–257.

Xin Z, Wang ML, Burow G, Burke J. 2009. An induced sorghum mutant population suitable for bioenergy research. Bioenergy Research **2**, 10–16.

Yu X, Li X, Guo T, Zhu C, Wu Y. 2016. Genomic prediction contributing to a promising global strategy to turbocharge gene banks. Nature Plants **2**, 1–7.

Zhang J, Ku LX, Han ZP, Guo SL, Liu HJ, Zhang ZZ, Cao LR, Cui XJ, Chen YH. 2014. The *ZmCLA4* gene in the qLA4-1 QTL controls leaf angle in maize (*Zea mays* L.). Journal of Experimental Botany **65**, 5063–5076.